Biotechnol Lett (2023) 45:799–809
https://doi.org/10.1007/s10529-023-03391-x

ORIGINAL RESEARCH PAPER

Physicochemical and histological analysis of an experimental endodontic repair material containing 45S5 bioactive glass

Michael Ranniery Garcia Ribeiro · Hudson Guterres Guilherme · Alina Neres Braga · Afonso Gomes Abreu · Érika Martins Pereira · Vandilson Rodrigues · José Bauer · Soraia de Fátima Carvalho Souza

Received: 1 February 2023 / Revised: 26 March 2023 / Accepted: 27 April 2023 / Published online: 6 May 2023

Abstract This study aimed to evaluate the maximum compressive strength, the modulus of elasticity, pH variation, ionic release, radiopacity and biological response of an experimental endodontic repair cement based on 45S5 Bioglass®. An in vitro and in vivo study with an experimental endodontic repair cement containing 45S5 bioactive glass was conducted. There were three endodontic repair cement groups: 45S5 bioactive glass-based (BioG), zinc oxide-based (ZnO), and mineral trioxide aggregate (MTA). In vitro tests were used to evaluate their physicochemical properties: compressive strength, modulus of elasticity, radiopacity, pH variation, and the ionic release of Ca^{+} and PO_4. An animal model was used to evaluate the bone tissue response to endodontic repair cement. Statistical analysis included the unpaired t-test, one-way ANOVA and Tukey's test. BioG showed the lowest compressive strength and ZnO showed the highest radiopacity among the groups, respectively ($p < 0.05$). There were no significant differences in the modulus of elasticity among the groups. BioG and MTA maintained an alkaline pH during the 7 days of evaluation, both at pH 4 and in a pH 7 buffered solutions. PO4 was elevated in BioG, peaking at 7 days ($p < 0.05$). Histological analysis showed less intense inflammatory reactions and new bone formation in MTA. BioG showed inflammatory reactions that decreased over time. These findings suggest that the BioG experimental cement had good physicochemical characteristics and biocompatibility required for bioactive endodontic repair cement.

Keywords Bioglass · Endodontics · Histological · Root resorption

M. R. G. Ribeiro
School of Dentistry, CEUMA University, Imperatriz, Brazil

M. R. G. Ribeiro · V. Rodrigues (✉) · J. Bauer · S. de Fátima Carvalho Souza
Dentistry Graduate Program, Federal University of Maranhão, Avenida dos Portugueses, 1966, Campus Universitário do Bacanga, São Luís, MA 65085-580, Brazil
e-mail: vandilson.rodrigues@ufma.br

H. G. Guilherme · A. N. Braga · É. M. Pereira
School of Dentistry, Federal University of Maranhão, São Luís, Brazil

A. G. Abreu
Graduate Program in Microbial Biology, CEUMA University, São Luis, Brazil

Introduction

Different approaches have been proposed for the treatment of external inflammatory root resorption (EIRR), and most of them have focused on procedures using intracanal materials (Heboyan et al. 2022). Calcium hydroxide pastes have been used as intracanal medication in cases of EIRR. However, the need for

periodic changes and long-term use may modify the mechanical properties of the root dentin (Ribeiro et al. 2017). Endodontic repair cement can be used as an alternative to calcium hydroxide pastes. The ideal repair cement for EIRR must be antibacterial, radiopaque, biocompatible, easy to handle, maintain an alkaline pH, and promote the repair of periradicular tissues (Parirokh and Torabinejad 2010b). In addition, compatible mechanical properties as such stiffness and strength are desirable for biomaterials that need to integrate with surrounding tissue and accelerate the healing of tissue damage (Arjunan et al. 2020, 2022).

Although direct occlusal stresses are rarely applied to repair cements used in endodontic procedures, resistance to compression is crucial for their handling and insertion into resorptive defects. Despite there being still no material with all of these characteristics, the Mineral Trioxide Aggregate (MTA) is currently considered the gold standard among the repair cements available on the market (Parirokh and Torabinejad 2010b). However, the difficulty of its manipulation and insertion into the appropriate sites, prolonged setting time, and dentin discoloration are disadvantages of this kind of cement (Parirokh and Torabinejad 2010a).

Previous research has suggested that alkaline bioactive glasses of the SiO_2–Na_2O–CaO–P_2O_5 system act as bactericides in infected root canals (Mehrvarzfar et al. 2011; Zhang et al. 2010). In addition to the bactericidal effect, bioactive glasses have bioactivity and remineralizing potential (Jung et al. 2022). Hydration of the bioglass particles causes the release of calcium, silica, phosphate, and sodium. That ionic release indirectly promotes an additional pH-related antibacterial effect (Mehrvarzfar et al. 2011). The adverse effects of bioglass on dentin mechanical properties appear to be less than those caused by calcium hydroxide and MTA (Natale et al. 2015; Ribeiro et al. 2017).

Among the existing types of bioglass, 45S5 Bioglass® stands out for being composed of molecular proportions of calcium oxides and phosphorus similar to those found in human bones (Krishnan and Lakshmi 2013). This bioglass has the ability to regenerate tissues, form hydroxyapatite and bind to hard tissues (Par et al. 2022; Cardoso et al. 2022). Chemically and structurally, hydroxyapatite is similar to human bone tissue. This allows osteoblasts to multiply in the hydroxyapatite layer that forms on the bioglass, establishing a strong connection with the bone tissue (Hench and Jones 2015). In vitro resorption models have shown that bioglass significantly inhibits the formation of osteoclasts and the expression of genes involved in bone resorption (Mladenović et al. 2014).

Associations of 45S5 with endodontic sealers and gutta-percha demonstrated effectiveness in apical sealing, greater Ca/P precipitation, and high pH induction (Heid et al. 2016). Despite this, there are scarce studies evaluating 45S5 as an endodontic repair cement (Washio et al. 2019; Cardoso et al. 2022). Because of the need for an effective bioactive material for the treatment of EIRR, this study evaluated the maximum compressive strength, the modulus of elasticity, pH variation, ionic release, radiopacity, and biological response of an experimental endodontic repair cement based on 45S5 Bioglass®.

Materials and methods

Study design and endodontic repair materials

This study was conducted to evaluate the in vitro physicochemical properties and in vivo bone tissue response using an animal model (Fig. 1). The experimental protocol was approved by the Ethics Committee on Animal Use of CEUMA University (no. 06/2017). The tests were performed on three endodontic repair material groups: 45S5 bioactive glass-based (BioG), zinc oxide-based (ZnO), and MTA.

The BioG experimental cement was prepared with 40% 45S5 bioactive glass (NovaBone Products, Alachua, FL, USA) and 60% zinc oxide (Sigma Aldrich, St Louis, MI, USA). The ZnO and MTA (Angelus, Londrina, SC, Brazil) cements were used at a 100% concentration as control groups. The BioG and ZnO cements were mixed with distilled and deionized water (DDW) at the proportion of 1:3, and weighed using a high-precision electronic balance (AD200 model, Marte, SP, Brazil). Table 1 summarizes the details of the main materials used in this study. The MTA cement was mixed according to the manufacturer's instructions. The materials were placed in polypropylene tubes (1.5 mL) and homogenized using a vortex for 1 min.

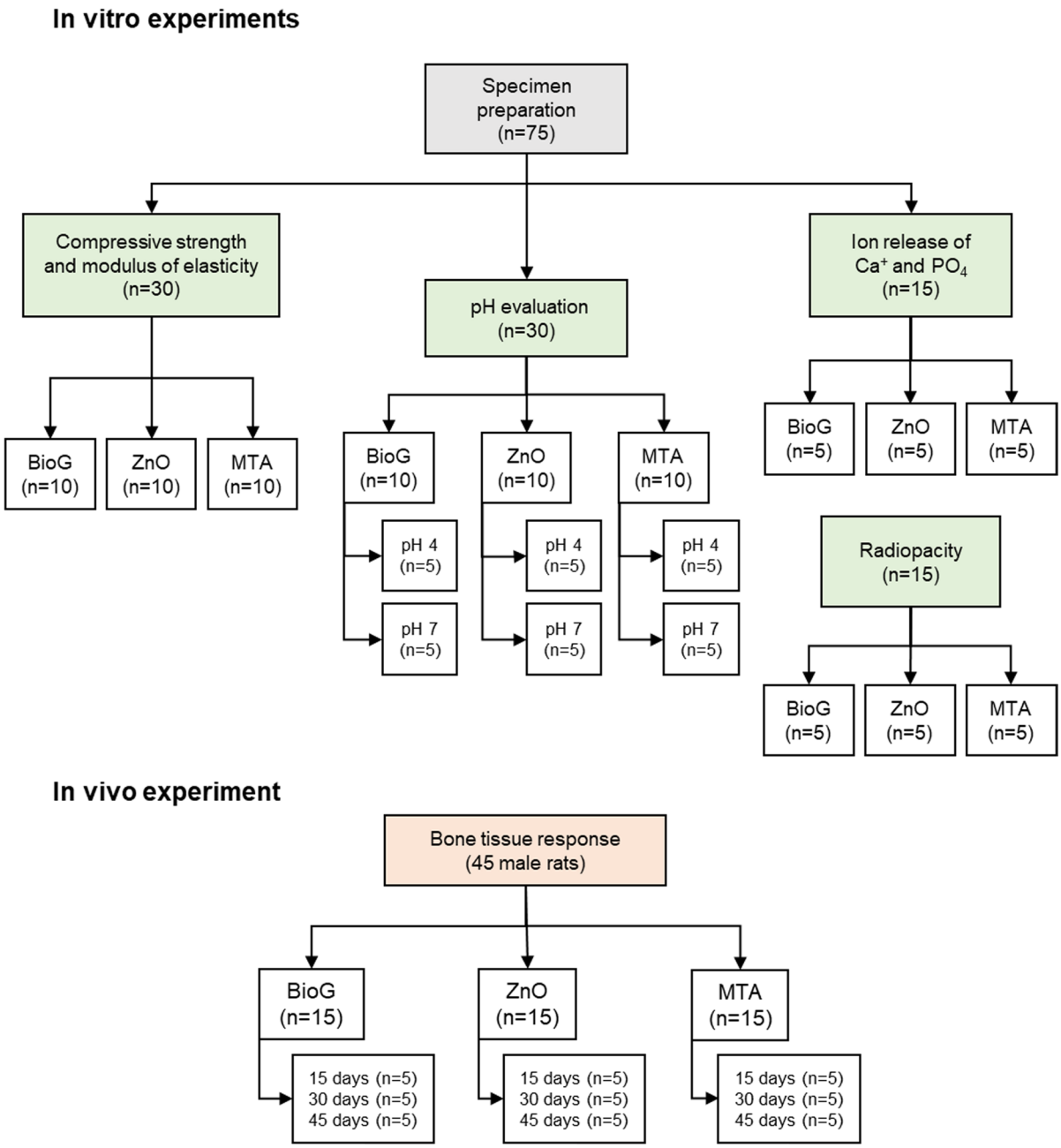

Fig. 1 Flowchart of the study

Specimens' preparation

Specimen preparation was made in a plastic matrix (12 mm × 6 mm Ø) according to the ANSI/ADA specification No. 66 (Mallmann et al. 2007), and distributed among the tests of maximum compressive strength, pH variation, and ionic release, in a total of 75 specimens (Fig. 1). A polyester strip was inserted below and above the matrix for packaging the materials and promoting surface smoothness. The cements were inserted in three increments interspersed with 1 min of vibration to avoid the formation of air

Table 1 Material, brand name, manufacturer, and composition of the main materials used in this study

Material (abbreviation)	Brand	Manufacturer (City, Country)	Composition
Bioactive glass (BioG)	45S5 Bioglass®	NovaBone Products (Alachua, USA)	45 wt% SiO_2, 24.5 wt% CaO, 24.5 wt% Na_2O, and 6 wt% P_2O_5
Zinc oxide (ZnO)	Zinc oxide—nanopowder	Sigma Aldrich (Saint Louis, USA)	ZnO nanoparticles (≤ 100 nm particle size)
Mineral Trioxide Aggregate (MTA)	White MTA	Angelus (Londrina, Brazil)	SiO_2, K_2O, Al_2O, Na_2O, Fe_2O, SO_3, CaO, Bi_2O_3, MgO, insoluble residues of CaO, KSO_4, $NaSO_4$ and crystalline silica

bubbles. After 24 h in an oven at 37 °C ± 1 °C and 100% humidity, they were removed from the dies and their edges were smoothed with sandpaper No. 1200 (Skill-Tec, São Paulo, SP, Brazil).

Compressive strength and modulus of elasticity

Thirty specimens were submitted to the compressive test (n = 10, per group) using a universal mechanical testing machine (Instron 3342, Canton, MA, USA) with a 50 N load and a speed of 0.5 mm/min. The compressive strength (in MPa) and modulus of elasticity (in GPa) values were calculated directly by the testing machine software.

Radiopacity

To determine the radiopacity, 3 acrylic matrices with 5 holes (1 mm × 10 mm Ø) were used to make the specimens (n = 5 per group). After conditioning, the cements were flattened with a glass plate overlay. The set was kept in an oven at 37 °C ± 1 °C and 100% humidity for 48 h. The thickness of the specimens was checked with a digital caliper (Mitutoyo, Tokyo, Japan), and the excess was removed with sandpaper No. 1200. An aluminum 12-step penetrometer (1 mm per step) was placed over the semi-direct digital plate sensor (Orion Corporation Soredex, Helsinki, Finland) to allow for analysis of the radiographic density. The radiographs were taken by an X-ray machine (Focus, Kavo Brasil, Joinville, SC) at 70 KVP and 7 mA, for 0.25 s with a 40 cm focus-film distance, according to specification No. 57 ANSI/ADA (Institute, 1984). After each exposure, the sensor was read on a Digora Optime® scanner (Orion Corporation Soredex, Helsinki, Finland). The images were exported to Kodak® Dental Imaging software to read the radiopacity in pixel values, ranging from 0 to 255. These values were converted to units in mm Al (Duarte et al. 2009).

pH measurements

Thirty specimens were used for this analysis (n = 10, per group). Buffering was carried out at pH 4 with hydrochloric acid and pH 7 with sodium hydroxide (n = 5, for each solution). Each specimen was immersed in 5 mL of solution and kept in a refrigerator at 4 °C ± 1 °C until reading. The pH values were measured using a digital pHmeter (Quimis Q400A, São Paulo, SP, Brazil) in triplicate at 15 min, 30 min, 1 h, 24 h, and 7 days after submersion (Xie et al. 2017).

Ion release of Ca^+ and PO_4

Fifteen specimens were used to determine the ion release of Ca^+ and PO_4 (n = 5, per group). After 24 h, 7 and 30 days submerged in 1 mL of DDW, 10 µL, and 100 µL aliquots were collected to measure Ca^+ and PO_4, respectively. Colorimetric analysis was performed in triplicate with Arsenazo III and Phosphomobilidate (Doles, Goiânia, GO, Brazil) by using a multiplate spectrophotometer (630 nm; Elx800UV, Biotek Instruments, Winooski, VT, USA) (Carvalho et al. 2016; Vogel et al. 1983).

Bone tissue response

The in vivo experiment included 45 male rats (Rattus norvergius, albinus, Wistar), aged approximately 8 weeks and weighing 300–400 g. The animals were conditioned in plastic boxes (dimensions, 37.5 × 32 × 16 cm^3) in a controlled-environment room (temperature, 23 °C ± 3 °C; humidity, 25%; light/dark cycle, 12/12 h). The animals received balanced feed

and water ad libitum. The animals were divided into three experimental groups (BioG, ZnO, and MTA), and each group was into three subgroups according to the experimental times (15, 30, and 45 days).

Anesthesia was performed with xylazine hydrochloride solution (Xilazin 2%, Syntec do Brasil Ltd.) and ketamine (Cetamin 10%, Syntec do Brasil Ltd.) Intramuscularly at a dose of 1.5 mL/kg. Then, trichotomy and asepsis were performed, followed by 1.0 cm incisions made parallel to the long axis of the right and left tibias. After syndesmotomy, a cavity 2 mm in diameter was made in the anterior wall of the right and left tibiae with a low rotation carbide bur, under saline irrigation. The cavity was filled with endodontic repair material (BioG, ZnO, or MTA) according to its group, and then the surgical wounds were sutured. A solution of iodinated polyvinylpyrrolidone was applied after suturing the surgical wounds. In the first 48 h after surgery, the animals received single daily intraperitoneal doses of 0.05 ml of injectable sodium dipyrone 500 mg/mL (Novalgina, Aventis Laboratory, Brazil).

At the end of each experimental period, the rats were euthanized in a gas chamber according to humanitarian techniques (SISBIO: 16716-1). The BioG, ZnO, and MTA animals were euthanized at 15, 30, and 45 days after the surgical intervention ($n=5$ per each subgroup).

A sample of each subgroup 1 cm equidistant from the endodontic material area was collected to serve as a control group. The tibial areas, where the material was filled during the surgical intervention, were removed and fixed by immersion in a 10% formaldehyde solution buffered in 0.1 M sodium phosphate buffer, pH 7.4 at 4 °C.

The samples were demineralized in a 10% EDTA solution for 30 days followed by routine histological processing. After this step, the specimens were embedded in paraffin and subjected to serial sectioning of 5 µm, followed by hematoxylin and eosin staining. Histological analysis was performed using a light microscope and Axio Vision Rel. 4.8 software (Carl Zeiss, Germany).

The area corresponding to the lower interface between the implanted material and bone was evaluated considering: the presence or absence of necrosis; the frequency and intensity of acute and chronic inflammatory cells (neutrophils, lymphocytes, macrophages, mast cells, plasmocytes, and giant foreign body cells); the formation and characteristics of a fibrous capsule around the implanted material; the possible resorption and replacement of the material by tissue; degeneration and disintegration along with inflammatory cells and blood vessels aspects.

Statistical analysis

The data analysis was conducted using GraphPad Prism version 9 (GraphPad Software Inc., San Diego, USA). Data are presented as mean values ± standard deviation. Normality assessments were performed using the Shapiro–Wilk test. Comparison analysis was performed using an unpaired t-test or one-way ANOVA and Tukey's tests. The significance level adopted was 5%.

Results

Compressive strength, modulus of elasticity, and radiopacity

Figure 2a shows the significant differences among the three groups ($p<0.05$). MTA presented the highest compression force while BioG was the lowest. There were no statistically significant differences in the elasticity module among the groups (Fig. 2b). In Fig. 2c, the radiopacity was higher in the ZnO than in the other groups ($p<0.05$).

pH evaluation

Figure 3 shows the variations of the pH values in the tested solutions. At pH 4 (Fig. 3a) and pH 7 (Fig. 3b), both BioG and MTA alkalized the medium, showing a more significant increase after the first 15 min ($p<0.01$), and the pH peaked after 7 days.

Ion release of Ca^+ and PO_4

Figure 4a illustrates the analysis of Ca concentration. There was a significant gradual increase in Ca^+ release in the BioG group during the analyzed period ($p<0.05$). The peak of Ca concentration in the MTA group occurred at 7 days ($p<0.05$). In the comparison among groups, MTA showed higher concentrations than BioG at both 24 h and 7 days ($p<0.05$).

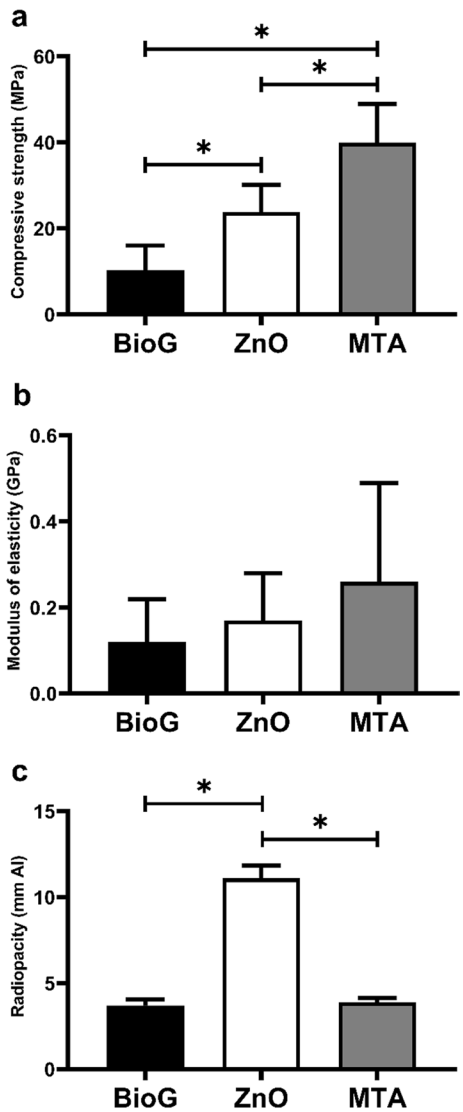

Fig. 2 Mean and standard deviation of the mechanical and radiographic evaluation of the groups. Maximum compressive strength (**a**), modulus of elasticity, (**b**) and radiopacity of the study groups after hydration and setting time (**c**). *Indicates statistically significant differences between the material groups ($p < 0.05$)

The PO_4 data are shown in Fig. 4b. In the BioG group, the 7 days and 30 days timepoints showed PO_4 concentrations statistically higher than at 24 h ($p < 0.05$). While in the MTA group, 30 days showed a statistically lower concentration than at previous times ($p < 0.05$). BioG compared to MTA showed a lower concentration at 24 h but it was higher at 7 days and 30 days ($p < 0.05$).

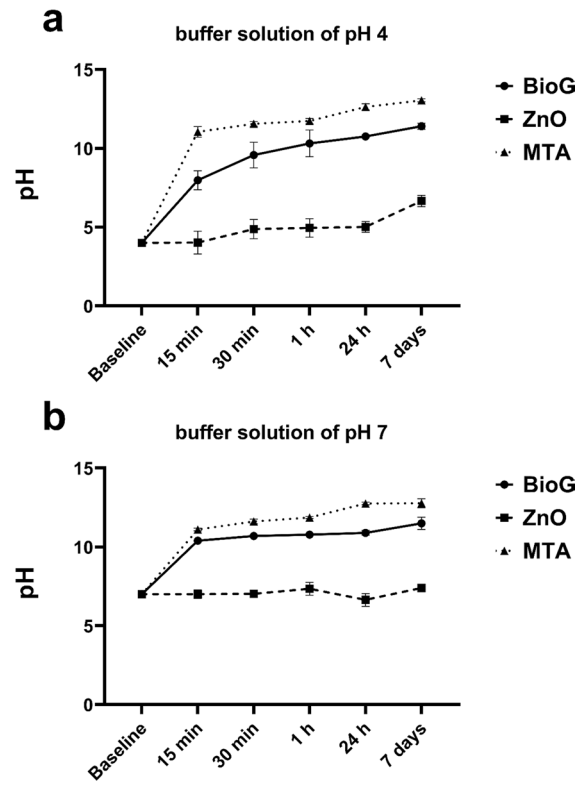

Fig. 3 Mean and standard deviation of the pH variation of the study groups in the buffered solutions (pH 4 and pH 7) at the experimental times

Histological analysis

Figure 5 illustrates representative regions of the histological sections in the study groups. The Control Group showed characteristics of integrity with osteocytes and matrix, and normality of the periosteum and medullary region. The BioG group presented with connective tissue and a larger number of blood vessels surrounding the material, the presence of an intense inflammatory infiltrate close to the bone surface region, without osteoclasts, bone marrow rich in connective tissue, inflammatory cells, and fibroblasts. In BioG over time, the material showed closer contact with the bone surface and at 45 days there was a reduction in the proportion of inflammatory cells. Internal erosion of the bioactive glass particles was not observed in any of the specimens. The ZnO group showed an intense inflammatory reaction during the entire period evaluated, with subtle resolution in the last period, congested blood vessels and a large

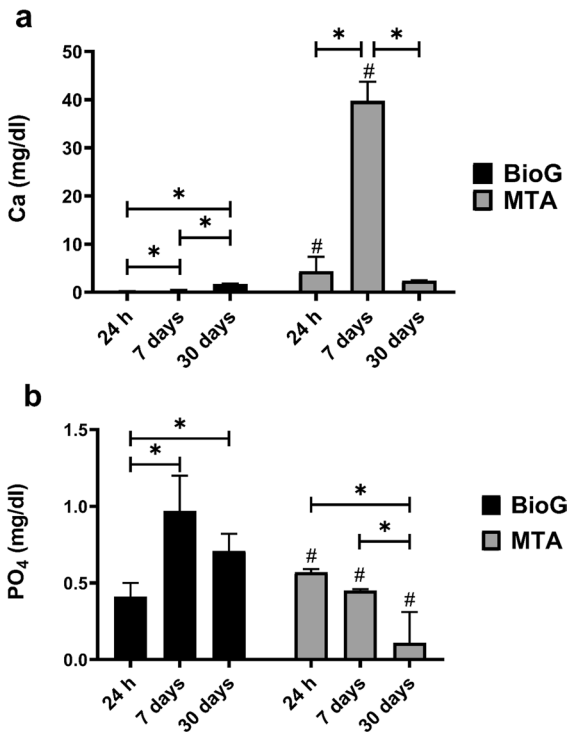

Fig. 4 Mean and standard deviation of calcium and phosphate concentration between the BioG and MTA groups and the evaluation period. *Indicates statistically significant differences between times in the same material group ($p < 0.05$). #Indicates statistically significant differences between materials at the same experimental time ($p < 0.05$)

number of inflammatory cells close to the material. In the MTA group, connective tissue was observed, rich in fibroblasts and collagen, inflammatory cells in small amounts covering the material, and with few blood vessels, the material in close contact with the bone tissue, and signs of bone neoformation.

Discussion

The main findings of this study, which compared maximum compressive strength, pH variation, and ionic release tests, among the BioG, ZnO, and MTA groups, suggest that the experimental endodontic repair cement at a 40% concentration of 45S5 has the required physicochemical requirements for a bioactive material.

The compressive strength of the endodontic repair cements varies according to the type of material and vehicle used, their proportion, the applied pressure, the mixing technique, and the storage conditions. These factors were considered in the standardization of the experimental groups. According to this study, the highest compressive strength values were recorded for MTA. This characteristic of MTA represents a disadvantage when it comes to the handling of this material and insertion into the location where it should act (Parirokh and Torabinejad 2010a). Although endodontic repair cements are not subjected to direct forces, they do experience compressive forces from intracanal insertion and masticatory mechanics. High compressive strength values similar to that of MTA can hinder the handling and maintenance of the cement in the resorptive cavity. On the other hand, it is believed that the formation of a superficial porous layer in Bioglass-based cements can reduce their compressive strength values, as noted in this study (Bellucci et al. 2011).

DDW was selected as a vehicle for BioG and ZnO cements because it provides faster ionic release of these materials. Eugenol is known to be a known vehicle for ZnO. However, despite the formation of zinc eugenolate being a factor that increases the strength of this cement, this vehicle was not used in this study because it is a genotoxic and mutagenic agent (Hunag et al. 2001). In this study, the physical evaluation of the cements, in all groups, presented low values of modulus of elasticity, which is expected for dental cements.

Evaluations of digital radiographic images using photodensiometry and aluminum scales have been previously performed (Carneiro et al. 2018; Duarte et al. 2009). Radiopacity is a crucial feature for endodontic filling materials to confirm the quality of the filling of the root canal system (Carneiro et al. 2018). Even without the inclusion of added opacifying agents, BioG obtained radiopacity values greater than 3 mm of Al, complying with specification No. 57 ANSI/ADA (Institute, 1984).

The radiopacity of the MTA is guaranteed by the addition of bismuth oxide. Camilleri et al. (2004) suggest that this radiopacifier affects the precipitation of calcium hydroxide released from the MTA and that it does not stimulate cell proliferation. In addition, bismuth oxide undergoes greater release when MTA is used under conditions of tissue inflammation (Parirokh and Torabinejad 2010b). Thus, the addition

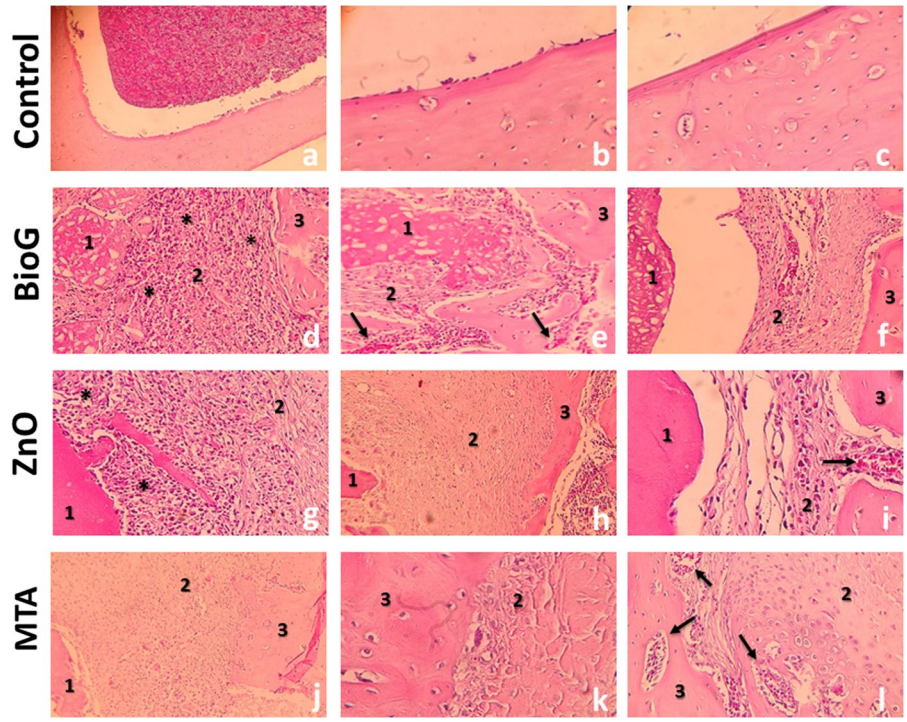

Fig. 5 Photomicrographs of histological sections of the bone regions and connective tissue surrounding the tested materials. Control group: (**a**, **b**, **c**; 50×, 100×, and 200×magnification). BioG: (**d**, **e**, **f**; 200×increase at 15, 30, and 45 days). ZnO: (**g**, **h**, **i**; 200×increase at 15, 30, and 45 days). MTA: (**j**, **k**, **l**; 200×increase at 15, 30, and 45 days). (1) Type of material, (2) Dense connective tissue, (3) Bone trabeculae, (*) Diffuse mononuclear inflammatory infiltrate, (→) Congested blood vessels

of bismuth oxide can reduce the biocompatibility of MTA.

BioG alkalized both the acidic and neutral medium, as well as releasing Ca and PO_4 over time. These results are consistent with that proposed by Cunha et al. (2011), who considered it desirable to increase the pH in the resorptive sites to neutralize the action of clastic cells. Thus, the ideal bioactive material should favor an increase in pH in the reabsorption area and remineralization of the reabsorbed area. Pieces of evidence have pointed out that the induction capacity of dentin remineralization gradually improves when an ionic release occurs (Rabiee et al. 2015). In addition, a previous study has shown that the 45S5 bioactive glass had the potential to neutralize acidic environments and induced the formation of hydroxyapatite precursors (Cardoso et al. 2022). In this in vitro evaluation, the BioG group reached its peak of Ca^+ and PO_4 release at 30 days, thus being slow and gradual. A rapid ionic release was observed in the MTA at 7 days, when it reached the peak of Ca^+ release and in the first 24 h for the release of PO_4. The saturation of these compounds, mainly Ca^+, as observed in the MTA, induces the formation of crystalline hydroxyapatite that does not participate effectively in tissue binding (Bingel et al. 2015).

Alkaline ions such as Na^+ and Ca^{2+} on the surface of the bioglass are exchanged for H+, causing hydrolysis of silica and changes in pH (Rabiee et al. 2015). The formation of hydroxyapatite is significantly faster in acidic challenges than in neutral ones due to the rapid ion exchange and the use of Ca^+ and PO_4 released from the bioglass (Cardoso et al. 2022). Concerning the release of Ca^+, the MTA showed a high ionic release of this compound associated with an increase in pH, being the highest among all groups. High pH values may not be as clinically desirable, as they induce negative changes in the mechanical properties of root dentin, which can lead to dental fractures (Ribeiro et al. 2017). Considering the strong increase in local pH promoted by MTA, we could assume that when indicated for the treatment of EIRR, it could cause negative changes in the dentinal structure (White et al. 2002). It is believed that an increase in pH just enough to paralyze the osteoclastic process is more advisable.

Histological analysis showed characteristics related to the formation of fibrous tissue involving the material in the BioG and ZnO groups. In the connective tissues adjacent to the bioglass particles, a moderate number of fibroblasts, macrophages, and lymphocytes are present. These results are similar

to those found by Melo et al. (2005). The formation of blood vessels related to the three experimental groups at 30 and 45 days, as well as the quantitative decrease in inflammatory cells over time, following the evidence available in the literature (Azenha et al. 2010). The excellent biocompatibility of 45S5 has already been demonstrated by Azenha et al. (2010) in Bioglass 45S5 implants in rabbit femurs, showing the bone formation and a layer of soft tissue in close contact with the implant surfaces in the spinal canal. In addition, a previous study has shown that bioactive glass-based root canal sealers can induce good wound healing of periapical tissues in clinical cases (Washio et al. 2019).

In both the BioG and MTA groups, the material had intimate contact with the bone tissue, with the formation of blood vessels in this connection. The areas in contact with BioG and MTA showed bone tissue closely related to the material particles, probably due to the osteoinductive property of these materials (Par et al. 2001). However, MTA was the only group that presented bone neoformation.

The MTA has a fast setting, even in a humid environment. In addition, the lack of membrane covering the filling materials could justify the lack of bone formation by BioG. This material has a considerable ionic dissociation rate, which can facilitate its dilution in the overlying connective tissue (Jones 2013). There was no new bone formation in the 45S5 Bioglass group. This finding can be explained by the short evaluation period (up to 45 days), which can be considered a limitation of our study. However, it must be considered that the repair of bone defects is achieved not only by the osteoconductive properties of bioactive glass granules but also by their osteostimulatory effect (Melo et al. 2005).

Moreover, pieces of evidence already have shown that BioG can activate genes that control osteogenic activity and growth factors, inhibit osteoclast formation and bone resorption, and stimulate the formation of hydroxyapatite and remineralization of dental hard tissues (Mladenović et al. 2014; Par et al. 2001). Furthermore, it is believed that BioG could also induce the repair of the defect caused by the EIRR (Mladenović et al. 2014).

Nevertheless, this study has some limitations. The in vitro design and in vivo animal model study can limit the interpretation and generalization of these findings to clinical practice. Another limitation was that the employed study design was limited to simulating the root canal environment. In addition, an immunohistochemistry analysis could detect inflammatory markers expression and clarify the tissue response to different materials. Therefore, future clinical studies with a larger sample, longitudinal design, therapy effect, and inflammatory markers are required to evaluate the long-term cost-effectiveness of endodontic repair material containing 45S5 bioactive glass.

Conclusion

The findings suggest that the experimental endodontic repair cement with a concentration of 40% of 45S5 Bioglass seems to be a promising material for the treatment of EIRR, as it presents the biocompatibility and resistance to being inserted in the root canal or applied in resorptive areas, can alkalize acid and neutral environments with the gradual release of PO_4 ions, which are involved in its bioactivity.

Author contributions MRGR: conceptualization, data curation, formal analysis, investigation, methodology, software, supervision, writing—review and editing. HGG: data curation, formal analysis, investigation. ANB: data curation, formal analysis, investigation. AGAJ: conceptualization, data curation, formal analysis, investigation, writing—original draft. ÉMP: formal analysis, investigation, methodology. VR: conceptualization, data curation, formal analysis, investigation, methodology, software, supervision, writing—review and editing. JB: formal analysis, investigation, methodology. SdFCS: conceptualization, data curation, formal analysis, funding acquisition, investigation, methodology, project administration, writing—review and editing.

Funding This work was supported by the Foundation for Research and Scientific and Technological Development of Maranhão (FAPEMA) [Grant number 01451/16], and the Coordenação de Aperfeiçoamento de Pessoal de Nível Superior Brasil (CAPES) [Finance Code 001].

Data availability The datasets generated during and/or analysed during the current study are available from the corresponding author on reasonable request.

Declarations

Conflict of interest The authors declare that they do not have any conflict of interest.

Ethics approval This study was approved by the Ethics Committee on Animal Use of CEUMA University (no. 06/2017).

References

ANSI (1984) American National Standards Institute. Specification no 57 for endodontic filling materials. J Am Dent Assoc 108:88

Arjunan A, Demetriou M, Baroutaji A, Wang C (2020) Mechanical performance of highly permeable laser melted Ti6Al4V bone scaffolds. J Mech Beh Biomed Mat 102:103517

Arjunan A, Baroutaji A, Praveen AS, Robinson J, Wang C (2022) Classification of biomaterial functionality. Encycl Smart Mat 1:86–102

Azenha MR, Peitl O, Barros VMR (2010) Bone response to biosilicates® with different crystal phases. Braz Dent J 21:383–389

Bellucci D, Cannillo V, Sola A (2011) A new potassium-based bioactive glass: sintering behaviour and possible applications for bioceramic scaffolds. Ceram Int 37:145–157

Bingel L, Groh D, Karpukhina N, Brauer DS (2015) Influence of dissolution medium pH on ion release and apatite formation of Bioglass® 45S5. Mat Let 143:279–282

Camilleri J, Montesin FE, Papaioannou S, McDonald F, Pitt Ford TR (2004) Biocompatibility of two commercial forms of mineral trioxide aggregate. Int End J 37:699–704

Cardoso OS, Meier MM, Carvalho EM, Ferreira PVC, Gavini G, Zago PMW, Grazziotin-Soares R, Menezes ASD, Carvalho CN, Bauer J (2022) Synthesis and characterization of experimental endodontic sealers containing bioactive glasses particles of NbG or 45S5. J Mech Beh Biomed Mat 125:104971

Carneiro KK, Araujo TP, Carvalho EM, Meier MM, Tanaka A, Carvalho CN, Bauer J (2018) Bioactivity and properties of an adhesive system functionalized with an experimental niobium-based glass. J Mech Beh Biomed Mat 78:188–195

Carvalho CN, Freire LG, de Carvalho APL, Duarte MAH, Bauer J, Gavini G (2016) Ions release and pH of calcium hydroxide–, chlorhexidine– and bioactive glass–based endodontic medicaments. Braz Dent J 27:325–331

Cunha RS, Abe FC, Araujo RA, Fregnani ER, Bueno CE (2011) Treatment of inflammatory external root resorption resulting from dental avulsion and pulp necrosis: clinical case report. Gen Dent 59:e101–e104

Duarte MAH, El-Kadre GDO, Vivan RR, Tanomaru JMG, Tanomaru-Filho M, Moraes IG (2009) Radiopacity of portland cement associated with different radiopacifying agents. J Endodont 35:737–740

Heboyan A, Avetisyan A, Karobari MI, Marya A, Khurshid Z, Rokaya D, Zafar MS, Fernandes GVDO (2022) Tooth root resorption: a review. Sci Prog 105:00368504221109217

Heid S, Stoessel PR, Tauböck TT, Stark WJ, Zehnder M, Mohn D (2016) Incorporation of particulate bioactive glasses into a dental root canal sealer. Biomed Glas 2:29–37

Hench LL, Jones JR (2015) Bioactive glasses: frontiers and challenges. Front Bioeng Biotech 3:194

Hunag TH, Lii CK, Kao CT (2001) Root canal sealers cause cytotoxicity and oxidative damage in hepatocytes. J Biomed Mat Res 54:390–395

Jones JR (2013) Review of bioactive glass: from Hench to hybrids. Acta Biomat 9:4457–4486

Jung MK, Park SC, Kim YJ, Park JT, Knowles JC, Park JH, Dashnyam K, Jun SK, Lee HH, Lee JH (2022) Premixed calcium silicate-based root canal sealer reinforced with bioactive glass nanoparticles to improve biological properties. Pharmac 14:1903

Krishnan V, Lakshmi T (2013) Bioglass: a novel biocompatible innovation. J Adv Pharm Technol Res 4:78–83

Mallmann A, Ataíde JCO, Amoedo R, Rocha PV, Jacques LB (2007) Compressive strength of glass ionomer cements using different specimen dimensions. Braz Oral Res 21:204–208

Mehrvarzfar P, Akhavan H, Rastgarian H, Soleymanpour R, Ahmadi A (2011) An in vitro comparative study on the antimicrobial effects of bioglass 45S5 vs. calcium hydroxide on *Enterococcus faecalis*. Iran Endodont J 6:29–33

Melo LGN, Nagata MJH, Bosco AF, Ribeiro LL, Leite CM (2005) Bone healing in surgically created defects treated with either bioactive glass particles, a calcium sulfate barrier, or a combination of both materials: a histological and histometric study in rat tibias. Clin Oral Imp Res 16:683–691

Mladenović Ž, Johansson A, Willman B, Shahabi K, Björn E, Ransjö M (2014) Soluble silica inhibits osteoclast formation and bone resorption in vitro. Acta Biomat 10:406–418

Natale LC, Rodrigues MC, Xavier TA, Simões A, De Souza DN, Braga RR (2015) Ion release and mechanical properties of calcium silicate and calcium hydroxide materials used for pulp capping. Int Endodont J 48:89–94

Par M, Gubler A, Attin T, Tarle Z, Tarle A, Tauböck TT (2022) Ion release and hydroxyapatite precipitation of resin composites functionalized with two types of bioactive glass. J Dent 118:103950

Parirokh M, Torabinejad M (2010a) Mineral trioxide aggregate: a comprehensive literature review-part I: chemical, physical, and antibacterial properties. J Endodont 36:16–27

Parirokh M, Torabinejad M (2010b) Mineral trioxide aggregate: a comprehensive literature review-part III: clinical applications, drawbacks, and mechanism of action. J Endodont 36:400–413

Rabiee SM, Nazparvar N, Azizian M, Vashaee D, Tayebi L (2015) Effect of ion substitution on properties of bioactive glasses: a review. Ceram Int 41:7241–7251

Ribeiro MRG, Thomaz ÉBAF, Lima DM, Leitão TJ, Bauer J, Souza SDFC (2017) Chlorhexidine prevents root dentine mineral loss and fracture caused by calcium hydroxide over time. Int J Dent 2017:1579652

Vogel GL, Chow LC, Brown WE (1983) A microanalytical procedure for the determination of calcium, phosphate and fluoride in enamel biopsy samples. Caries Res 7:23–31

Washio A, Morotomi T, Yoshii S, Kitamura C (2019) Bioactive glass-based endodontic sealer as a promising root canal filling material without semisolid core materials. Materials 12:3967

White JD, Lacefield WR, Chavers LS, Eleazer PD (2002) The effect of three commonly used endodontic materials on the strength and hardness of root dentin. J Endodont 28:828–830

Xie X, Wang L, Xing D, Zhang K, Weir MD, Liu H, Bai Y, Xu HHK (2017) Novel dental adhesive with triple benefits

of calcium phosphate recharge, protein-repellent and antibacterial functions. Dent Mat 33:553–563
Zhang D, Leppäranta O, Munukka E, Ylänen H, Viljanen MK, Eerola E, Hupa M, Hupa L (2010) Antibacterial effects and dissolution behavior of six bioactive glasses. J Biomed Mat Res Part A 93:475–483